C. R. Physique 11 (2010) 265–273

Contents lists available at ScienceDirect

Comptes Rendus Physique

www.sciencedirect.com

Computational metallurgy and changes of scale / Métallurgie numérique et changements d'échelle

Modeling grain growth and related phenomena with vertex dynamics

Modélisation de la croissance de grains par dynamique de vertex

Joël Lépinoux [a,*], Daniel Weygand [b], Marc Verdier [a]

[a] *SIMaP, INPG, CNRS, UJF; campus Grenoble, 38042 St Martin d'Hères, France*
[b] *Karlsruhe Institute of Technology (KIT), izbs, Kaiserstr 12, 76131 Karlsruhe, Germany*

ARTICLE INFO

Article history:
Available online 24 August 2010

Keywords:
Grain growth
Mesoscopic scale
Numerical simulations
Vertex dynamic model

Mots-clés :
Croissance de grains
Échelle mésoscopique
Simulation numérique
Dynamique de vertex

ABSTRACT

Grain growth is the simplest phenomena related to the evolution of a population of grains in crystalline materials. Some typical results obtained with vertex dynamics, a deterministic technique applied to the simulation of grain growth in polycrystalline materials, mostly in two dimensions (2D), are presented: (i) the dynamics of a population of grains interacting with various distributions of pinning obstacles; (ii) bulging as a possible recrystallization mechanism; and (iii) the influence of a confined geometry on grain growth as those found in electronic devices. Finally recent developments in 3D are presented.

RÉSUMÉ

La croissance de grains est le plus simple des phénomènes liés à l'évolution d'une population de grains dans les matériaux cristallins. Une technique de simulation numérique déterministe developpée à la fin des années 1990, la dynamique de vertex, est bien adaptée à cette classe de problèmes impliquant un grand nombre d'objets élémentaires connectés. Quelques cas d'étude sont présentés afin d'illustrer ce qui peut être appris avec cette technique de simulation.

1. Introduction

In polycrystalline materials, grain boundaries (GBs) are the interfaces which separate regions of different crystalline orientation of size ranging from about ten nanometers to macroscopic sizes. Considered as structural defects from a crystalline point of view they greatly influence various physical (electronic transport, mechanical response…) and chemical properties (corrosion) [1,2]. Their structure and their interaction with other defects inherent to polycrystalline materials like dislocations or precipitates have been the goal of numerous studies at the atomic scale. Nevertheless from a quantitative point of view, their mesoscopic properties (mesoscopic being a scale bridging the atomic level to a continuum description) are still very poorly known, except in few materials, which is a major concern to feed simulations with reliable data.

Grain growth is the simplest phenomenon concerning the evolution of a grain population at a mesoscopic scale; it involves only the interface energy of GBs. The driving force being the reduction of the total interface energy, GBs move toward their center of curvature. On the contrary, recrystallization is driven by the deformation energy stored inside the

* Corresponding author.
E-mail addresses: Joel.Lepinoux@simap.grenoble-inp.fr (J. Lépinoux), daniel.weygand@izbs.uni-karlsruhe.de (D. Weygand).

1631-0705/$ – see front matter
doi:10.1016/j.crhy.2010.07.015

volume of grains. Thus, in this case, the competition of reduction of stored energy between neighboring grains may lead GBs to move either in or opposite to their center of curvature.

To study all these phenomena in three dimensions (3D) the type of objects one has to handle are: volumes (i.e. grains G), interfaces (i.e. faces F), lines (i.e. edges E) and points (i.e. vertices V). In 3D, these quantities are linked by the so-called Euler equation which writes: $V - E + F - G = 1$. Obviously, grain growth and related phenomena are much easier to model and analyze in 2D than in 3D, but some aspects of grain coarsening in bulk materials can be investigated only in 3D. This is why, historically, all developments and simulation techniques of this class of phenomena have been first developed in 2D then extended in 3D if possible.

This article aims at giving a simple overview of a deterministic simulation technique, called vertex dynamics (belonging to the so-called front-tracking simulation method solving partial differential equations), and to illustrate the capabilities of this method with some typical problems in physical metallurgy and major concerns in industrial applications, namely the interaction with pinning particles, the occurrence of bulging in deformed materials, and for more recent works, its application to complex confined geometries with nanograins. Finally, the development of a reliable 3D simulation scheme, likely to be applied to a wide range of problems out of reach until recently is presented.

2. Physical principles

The vertex dynamics model described here was developed by Weygand et al. [3–8] starting from the work of Kawasaki's group [9,10]. In 3D, GBs are triangulated while in 2D edges are discretized into linear segments, the physical principles being the same: the evolution of the microstructure is described by the displacement of the nodes (vertices) needed for the discretization of the grain boundaries. The displacement of triple nodes in 2D, quadruple nodes in 3D follow the same law. Here we detail the formalism when the driving force for grain coarsening is solely due to the reduction of interface energy.

The approach is written in form of a potential – total interfaces energy – and a dissipation power due to the motion of the interface. The potential energy of the system is then defined by the functional:

$$V\big(\{\vec{r}\}\big) = \int_{\mathrm{GB}} \gamma(a)\,\mathrm{d}a$$

where a is the curvilinear coordinate along the GBs, $\gamma(a)$ the interface or grain boundary energy (here taken isotropic but it might be set dependent on the difference of orientation from part to part of the GB or the local inclination of the interface) and $\vec{r}$ is the vector field of vertices positions required for the interface discretization.

The displacement of GBs induces dissipation described by the functional R. In this particular description a linear relationship between the local velocity and the friction is assumed, leading to the following dissipation potential:

$$R\big(\{\vec{r}\},\{\vec{v}\}\big) = \frac{1}{2}\int_{\mathrm{GB}} \frac{v^2}{m_{\mathrm{GB}}}\,\mathrm{d}a$$

Here $\vec{v}$ is the vector field of local vertices velocities, v is the velocity normal to the GB area da of mobility m_{GB}. These integrals are calculated as discrete sums over elementary triangles in 3D, or linear segments in 2D. Then using the Lagrange equation

$$\frac{\partial V(\{\vec{r}_n\})}{\partial \vec{r}_i} + \frac{\partial R(\{\vec{r}_n\},\{\vec{v}_n\})}{\partial \vec{v}_i} = 0 \quad i,n = 1,\ldots,N$$

where N is the total number of vertices, a system of coupled equations is derived from which the velocity of each vertex is calculated:

$$D_i\vec{v}_i + \frac{1}{2}\sum_{j,k}^{(i)} D_{(ijk)}(\vec{v}_i + \vec{v}_k) = \vec{f}_i \quad i,j,k = 1,\ldots,N$$

where the double sum (j,k) is running over vertices connected to vertex (i). In 3D, we denote $A_{[ijk]}$ the surface of the triangle defined by the three vertices at positions $\vec{r}_i$, $\vec{r}_j$ and $\vec{r}_k$, with the convention $\vec{r}_{[ij]} = \vec{r}_i - \vec{r}_j$; $A_{[ijk]}$ writes:

$$A_{[ijk]} = \frac{1}{2}\|\vec{r}_{[ik]} \times \vec{r}_{[jk]}\|$$

The matrices D_i and $D_{(ijk)}$ are respectively defined by:

$$D_i = \sum_{j,k}^{(i)} D_{(ijk)}$$

$$D_{(ijk)} = \frac{A_{[ijk]}}{6\mathrm{m}_{\mathrm{GB}[ijk]}}\vec{n}_{[ijk]} \otimes \vec{n}_{[ijk]}$$

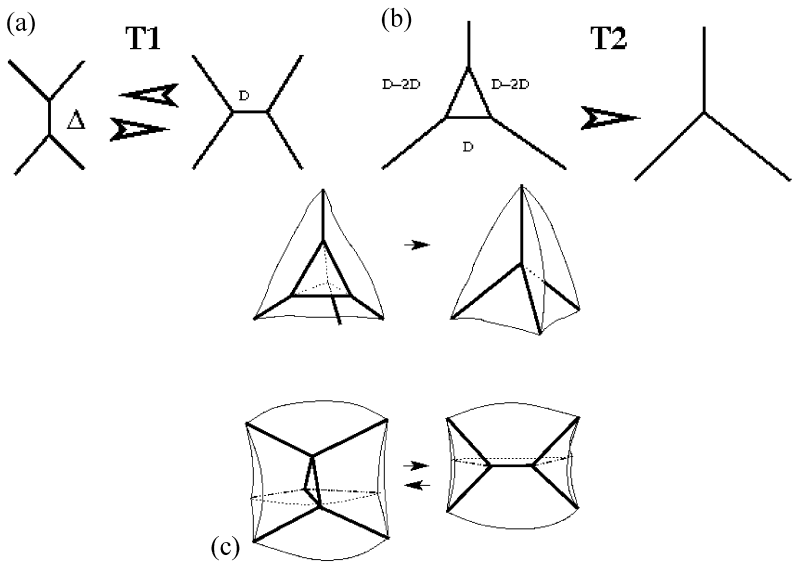

Fig. 1. Elementary topological transformations in 2D (a–b, called T1 and T2, respectively) and in 3D (c).
Fig. 1. Transformations topologiques élémentaires en 2D (T1 et T2) et en 3D.

with

$$\vec{n}_{[ijk]} = \frac{\vec{r}_{[ik]} \times \vec{r}_{[jk]}}{\|\vec{r}_{[ik]} \times \vec{r}_{[jk]}\|}$$

while f_i is defined by

$$\vec{f}_i = \frac{1}{2} \sum_{j,k}^{(i)} \gamma_{[ijk]} \vec{n}_{[ijk]} \times \vec{r}_{[jk]}$$

and $\gamma_{[ijk]}$ and $m_{GB[ijk]}$ are the local grain boundary energy and mobility of the triangle with area $A_{[ijk]}$.

The above formalism can be extended to include various ingredients for physical description of GBs motion such as triple line drag [7,8] or inclination dependent grain boundary properties [11]. The discretization of GBs in 2D has to be fine enough to naturally allow the GB to bow and to reach the condition of local equilibrium at triple nodes, i.e. 3 angles of 120° in the case of isotropic GB energy (see Section 3 for 3D), whereas the overall growth kinetics was found to be rather insensitive to the discretization [3,11]. It is important to note that in the vertex model, the equilibrium condition at triple lines is an outcome and not a boundary condition as in many sharp interface models [12,13].

Compared with other simulation techniques, in particular Phase Field, Vertex Dynamics is a very fast and flexible method in which various new ingredients or properties related to the interface including the triple lines can be readily introduced without modifying the global formalism. Comparisons of normal grain growth done on small population of grains in 2D showed that both techniques lead to the same overall results in isotropic conditions [14]. The overall dynamics can be scaled rigorously to coincide for both models. The topology and topological changes, inherently handled in phase field models, occur in rather similar manner: a two dimensional test system of initially 100 grains showed the first topological differences after loss of more than 50% of the initial grain population. Nevertheless there was a factor of more than two orders of magnitude in computing time in favour of the vertex dynamics model. Furthermore it seems more difficult to impose anisotropy, for both surface energy and GBs mobility or a supplementary triple line or quadruple point drag, ingredients which are easily introduced in vertex dynamics as functions of the local crystalline misorientation [3–8,11] or supplementary dissipation terms [7,8]. On the other hand, phase field model description can in principle easily be coupled to volume properties, e.g. elastic properties and interfacial properties, within the computational resources available [15,16].

Vertex dynamics is a fast algorithm but the price to pay is the difficulty to solve topological transformations. Indeed, contrary to phase field methods, GBs are discrete and sharp boundaries and in principle various types of topological events have to be described. Fig. 1 illustrates some idealized examples of such topological transformations in 2D and 3D. A detailed description of the implementation of these transformations in three dimensions is given in [4,11]. The transformation can be reduced to simple merging and splitting routines of real vertices, based on the local forces.

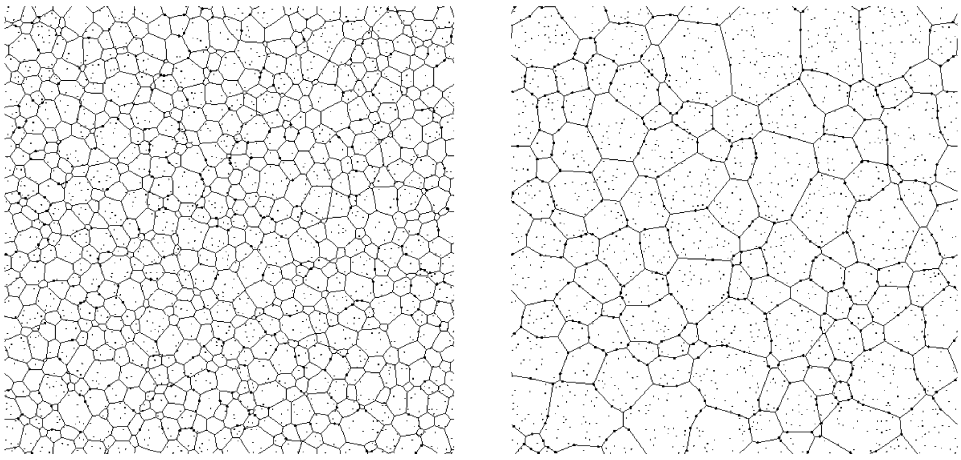

Fig. 2. Evolution of a grain structure: $F_{cr} = \gamma/2$, 2000 particles. (left) Early state (722 grains); (right) saturation (127 grains).
Fig. 2. Evolution d'une structure de grains avec $F_{cr} = \gamma/2$ et 2000 particules. (à gauche) État initial, 722 grains ; (à droite) état final à saturation, 127 grains.

3. Results

3.1. Pinning particles

Grain size of polycrystalline materials is one of the key microstructural length scales to control their mechanical properties. For a given size of structure, it is the only length scale which can be set within a wide range of possible values. Controlling the grain size and its stability with time is one of the common tasks of metallurgists. For that purpose a simple way consists in adding to the alloy a solute element of small solubility limit at temperature of use, to obtain precipitates able to pin the GBs, well known as the Smith–Zener pinning [17]. An overview on different modelling approaches can be found in [18]. To describe the interaction between such a pinning center and a GB, the important physical parameters are the volume fraction f of particles and, in 3D, their size r. Due to the complexity of the three dimensional system, as explained in the sharp interface model describing the pinning of a single grain boundary in 3D [19], this problem was first analyzed in 2D [5]. To mimic the three dimensional case in 2D a particle distribution with a density N and a strength F_{cr} was studied. The use of a pinning strength relates to the observation, that in 3D the size of the precipitate matters but not in a 2D case. The condition for unpinning in the 2D equivalent derives simply from the definition of a critical angle Φ_c such that $\sin(\Phi_c) = F_{cr}/2\gamma$ [3]. Such pinning of GB population is a typical example of so-called "collective pinning problems" [20]. From a practical point of view, particles pinning GBs are handled as special vertices. Topological transformations involving such vertices require of course special attention.

The simplest situation to investigate is a random distribution of particles of identical strength [3]. Fig. 2 shows an early configuration and the saturation state in which all GBs are pinned, i.e. when the capillary force equals the pinning force. Assuming that the (collective) pinning force remains constant during the evolution and equal to γ/R_{max}, one can write a simple phenomenological law for the evolution of the average grains size:

$$\frac{\mathrm{d}R}{\mathrm{d}t} = \alpha m_{\mathrm{GB}} \gamma \left(\frac{1}{R} - \frac{1}{R_{max}} \right)$$

R_{max} is the average radius of grains when the structure is pinned and α is a constant about 0.3, a value which slightly depends on F_{cr}. Fig. 3 shows that the assumptions used to write the above equation are correct: the predicted curve is in good agreement with simulation results and the normalized behavior does not depend on N for a given value of F_{cr}. The knowledge of the average size is not always sufficient to correctly predict all properties of such granular distributions. It is also important to characterize the whole distributions which fit very well a log-normal law, with a mean square deviation depending on the pinning force. The smaller the pinning force, the sharper the distribution (cf. Fig. 4) [3].

The number of particles found along GBs at saturation has been found to be related to the pinning strength of particles in a very simple way: $n_{\mathrm{GB}} \approx 3.26\gamma/F_{cr}$ [3]. Using simple arguments it was shown *a posteriori* that the proportionality factor is expected to be about π (for triangular grains) a value very close to the obtained one. For moderate pinning forces, the mean area at saturation (πR_{max}^2) was found to scale with $1/NF_{cr}^{2.8}$; the force exponent is close to that predicted by Hazzeldine following Friedel statistics, i.e. 3 [21]. These results are typical examples of the ability of vertex dynamics to reveal new features or to explore the predictions of analytical models.

Despite the 2D limitation, the flexibility of vertex dynamics is powerful to investigate the effect of various ingredients, for instance the type of spatial distribution of particles. Indeed, in practice, depending on metallurgical processes, pinning particles are often distributed in bands or clusters. Fig. 5 shows examples of final configurations for these two cases. From

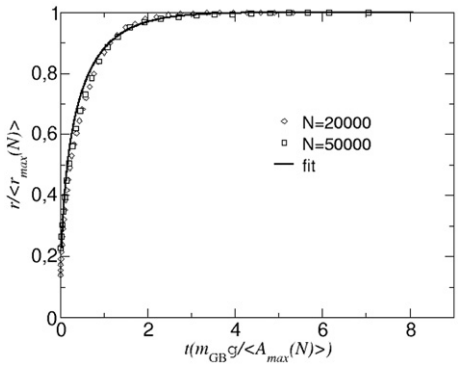

Fig. 3. The grain growth dynamics for $F_{cr} = \gamma/4$ and two particle densities. In the time unit, $\langle A_{max}(N)\rangle$ is the average saturation grains area for N particles in the considered system.

Fig. 3. Dynamique de croissance de grains pour $F_{cr} = \gamma/4$ et deux densités de particules. Dans l'unité de temps, $\langle A_{max}(N)\rangle$ est la taille moyenne de grain à saturation pour N particules dans le système.

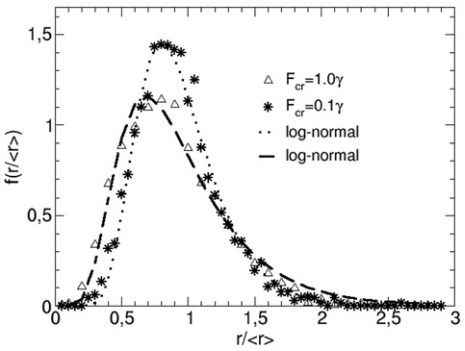

Fig. 4. The grain size distribution of pinned GB microstructures for 2 different pinning forces.

Fig. 4. Distribution de taille de grain des structures de grains ancrés pour 2 forces d'ancrage.

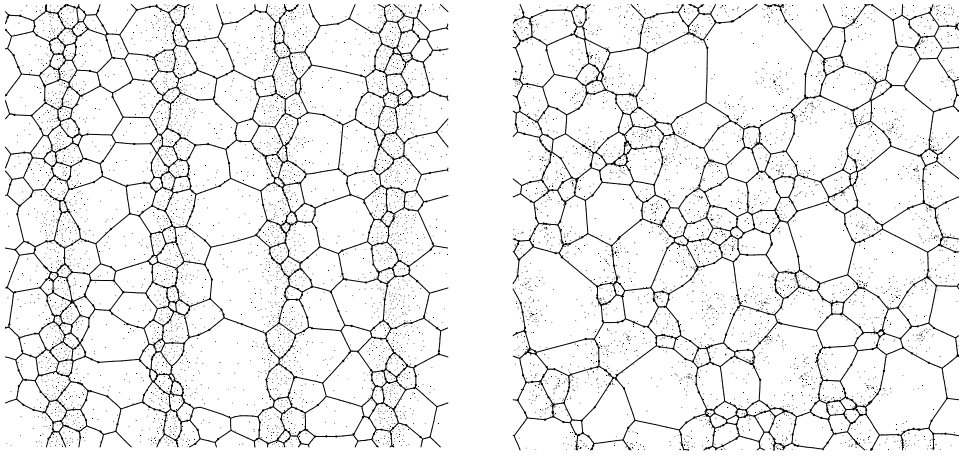

Fig. 5. Examples of pinned structures for heterogeneous distributions of particles, in bands (left) and clusters (right).

Fig. 5. Exemples de structures épinglées pour des distributions hétérogènes de particules, en bandes (à gauche) et en amas (à droite).

the comparison with random distributions of same strength, the pinning efficiency of these three types of distributions leads to: $A_{max}(\text{random}) < A_{max}(\text{band}) < A_{max}(\text{cluster})$.

In a given alloy, not only all particles do not have the same size but their nature can also be different, thus in general, the pinning force is not as simple as described here. This can be easily investigated with vertex dynamics using for instance two distributions of particles of different pinning strength and same concentrations to ease the analysis. The result writes:

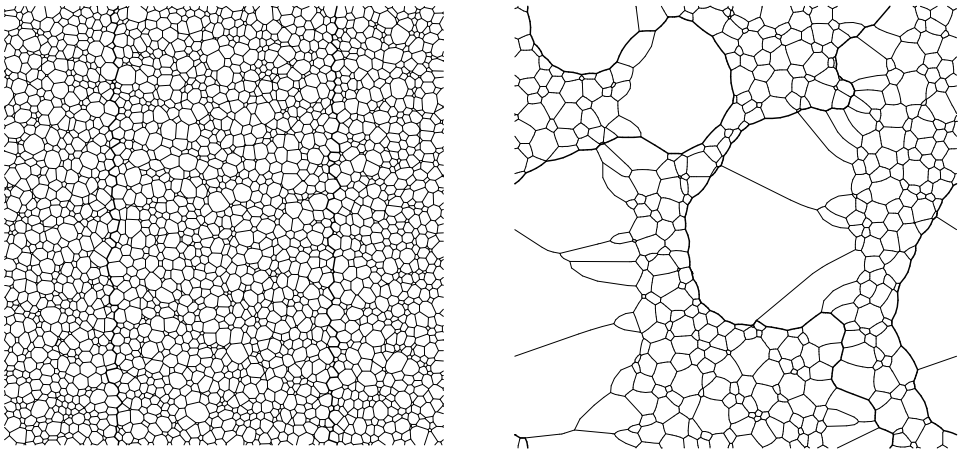

Fig. 6. Isotropic case. HGBs (bold lines) and LGBs (thin lines), same average subgrain size from part to part of HGBs. Initial state (left) and bulging (right).

Fig. 6. Cas isotrope. Joints de grains (en gras) et sous-joints de grains (ligne fine), même taille de sous-grain de part et d'autre des joints de grains initiaux. Etat initial (à gauche) et formation par gonflement de germes de grains (à droite).

$$\frac{1}{R_{max}^2} = \left(\frac{1}{R_{max,1}^2} + \frac{1}{R_{max,2}^2} \right)$$

an equation which can be easily generalized to any kind of particle distribution.

3.2. Bulging

The nucleation of recrystallization, i.e. how new well-defined grains appear in extensively deformed crystalline materials, is another classical problem in metallurgy. Bulging is a possible mechanism proposed by Bailey and Hirsch [22]; it suggests that recrystallization starts at former GBs in the deformed structure by nucleation of bulges. However, the size of these bulges and the relation with the local structure remain open questions. This is another example of using vertex dynamics to test assumptions and predictions of analytical models.

To investigate this problem we used a GB of high energy (HGB) and mobility (a former GB of the initial structure before deformation), separating two regions of subgrain sizes d_1 and d_2, subgrains being defined as GBs of low energy and mobility (LGB). The ratio of energies was about 1.6 and that of mobilities about 20. With $d_1 = d_2$, bulging results as local fluctuations of the HGB, as shown in Fig. 6.

On the contrary, with a size gradient (a trick to mimic a difference in stored energy) from part to part of the HGB, instead of bulging a fairly homogeneous columnar growth or interfacial subgrains was observed inducing the translation of the HGB [4]. Basically the same behavior was observed with anisotropic conditions, surface energy and mobility depending on the misorientation; however bulging was found more probable than with isotropic conditions in the case of a size (strain) gradient. Nevertheless, these comparisons suggest that bulging is more likely to occur inside heavily deformed regions than at the interface between zones of high and low deformation where the migration of the interface is the dominant mechanism.

3.3. Grain growth in nanomaterials with confined geometry

The improvement of global performances in semiconductor devices is limited by the increase of resistivity in metallic line of 3D interconnects (typically *fcc* metal). Therefore, the control of the evolution of grain boundaries structures in complex geometries is required. As a first step, this problem was investigated in 2D, first in films of finite width then in Damascene geometries, i.e. a film connected to a line of finite depth and width, called via. One of the new ingredients in this problem is the presence of specific interfaces (in reality, layers of diffusion barrier), e.g. the borders between the film and the substrate or the surface. The surface energy of GBs along such interfaces depends on the orientation of their cut plane, thus the texture of orientations versus the normal of interfaces is likely to be an important feature. This point has been investigated in a simple way first within films and by giving a surface energy advantage to grains well oriented along a ⟨111⟩ axis normal to the borders of the film, to mimic the fact that *fcc* grains along higher surface energy materials (nitride, refractory metals…) usually adopt this dense plane [2,23,24]. Depending on the value of the interface energy advantage given to well-oriented grains for a given ratio of the band width and the mean grain size, the ⟨111⟩ texture can vanish or on the contrary develop as shown in Fig. 7 [25].

The next step is more complex due to the "T" geometry of the Damascene structure shown in Fig. 8. Indeed, the fact that the orientation of borders is no longer constant requires to describe the structure with a set of linear segments of various

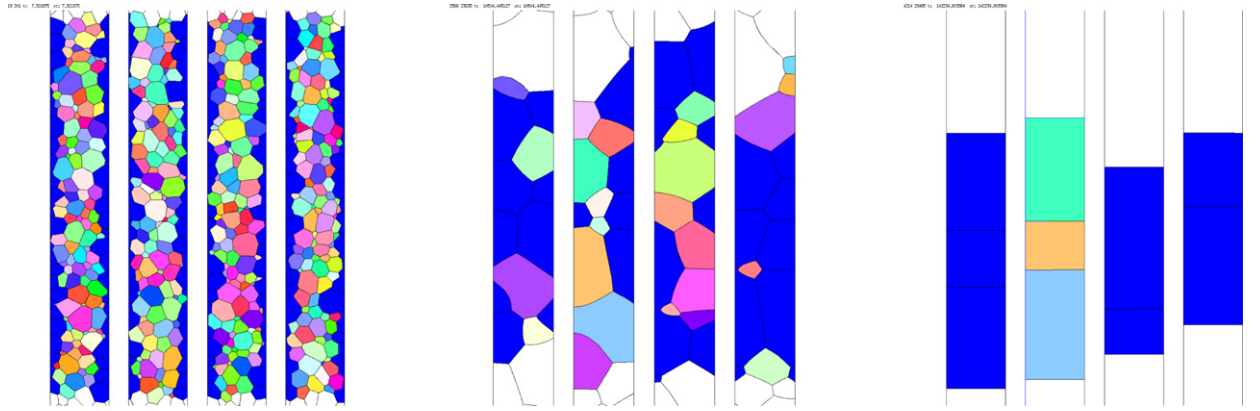

Fig. 7. A typical sequence for four bands with a {111} texture (grains in blue) along interfaces. Except in one band, well-oriented grains invade the band. The average final size of bamboo cells is about 5/3 of the width of bands. Grains concerned by periodic boundary conditions are not coloured.

Fig. 7. Evolution de la structure de grainsentre deux interfaces dans un film avec une texture {111} (en bleu). Hormis dans une bande, les grains bien orientés envahissent la bande. La taille moyenne finale est d'environ 5/3 de la largeur du film. Les grains qui subissent les conditions périodiques ne sont pas coloriés.

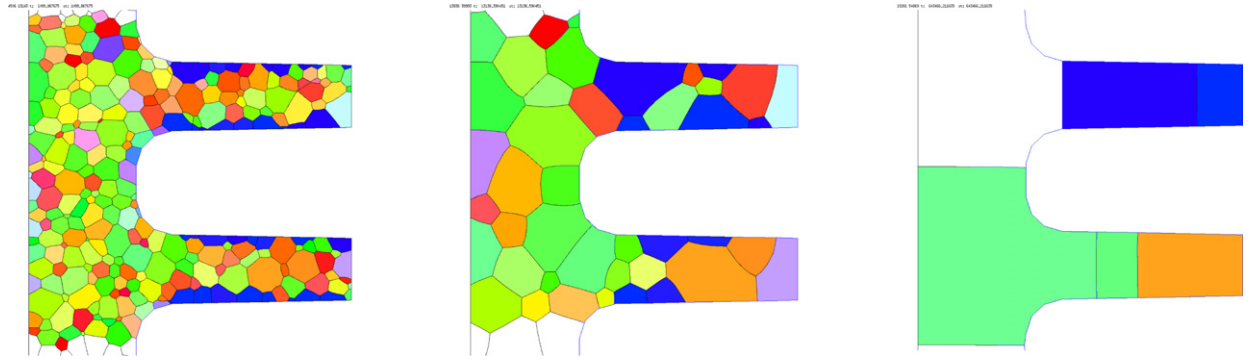

Fig. 8. A typical example of evolution of grains in the Damascene geometry with a {111} texture normal to via edges (in blue).

Fig. 8. Exemple d'évolution de microstructure de grains dans une structure Damascene avec une texture {111} normale aux parois du via (en bleu).

lengths, in particular in the region they are curved. Topological transformations along such interfaces have been the main difficulty to overcome [18].

Now it becomes necessary to monitor the texture along the two main directions, i.e. the X and Y axis. In Fig. 8, only the component along the direction normal to the via walls (the via is this finite depth line seen end-on, connected to the film) is monitored. It shows that the ⟨111⟩ component might fill the lines but not always; again it depends on the interface energy advantage given to the ⟨111⟩ texture as well as of the various geometrical features [18].

3.4. Recent developments in 3D

For the general case of anisotropic grain boundary properties the discretization of the modeled microstructure has to be adaptive to represent the anisotropic properties precise enough. A detailed description of the refined three dimensional vertex model, allowing for an arbitrary refined interface triangulation, can be found in [11]. Only the main features and validation of the new model are given here. Both the geometrical and physical description of the vertex model is improved. A triangulation scheme, with local refinement is developed, including a generalized scheme for topological changes. A set of rules for collapsing and decomposing real vertices based on force and energy criteria is defined. As shown in Fig. 9, the grain structure consists of vertices of two kinds, so-called real vertices, which are topological necessary discretization nodes, connecting triple lines and virtual vertices, either located within a grain boundary or along the triple lines, which serve as discretization points only. Connected vertices with a distance smaller than a critical length are merged. Real vertices, connected to more than 4 triple lines are allowed to decompose in separate real vertices, depending on the forces due to the attached grain boundaries [11]. No artificial limitations on the number of triple lines connected to a real vertex or number of grain boundaries shared by a “triple” line exists. The physical properties of a GB may now depend on the local misorientation and the local grain boundary inclination. The latter dependency introduces a torque force contribution to the nodal forces, stabilizing low energy grain boundary inclinations.

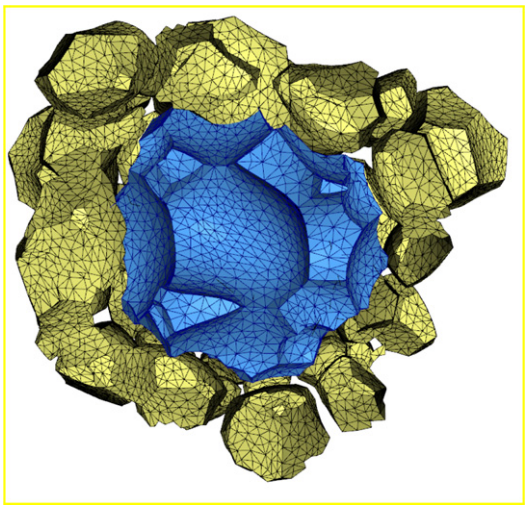

Fig. 9. An abnormally growing grain (within the modeled growth time) in the center is shown with a selection of neighboring grains of the matrix shifted along the direction connecting the respective grain centers. The central grain has a 30% lower grain boundary energy compared to the matrix and a mobility which is three times larger.

Fig. 9. Croissance anormale d'un grain (à l'echelle de la durée de la simulation), au center, entouré de ses voisins, translatés suivant la direction joignant leurs centres. L'énergie d'interface de ce grain est 30% plus faible que celle de ses voisins tandis que sa mobilité est trois fois plus élevée.

In Fig. 9, a grain with its surrounding matrix grains are shown, clearly revealing the curved grain boundaries and the strongly bended triple lines, between the quadruple points. The shown structure is grown under anisotropic conditions, the central grain exhibiting an interface energy of 0.7 of the matrix interface energy and a GB mobility three times larger than the one of matrix GBs.

Under normal grain growth conditions, the observed grain growth dynamics in the new model was found to be within the uncertainties of the "poorly" discretized old model [4], indicating that changing the discretization of the interfaces in the vertex dynamics approach does not alter the overall growth dynamics [11]. Despite these observations on the growth dynamics, a linear relation between an equivalent area versus time [4,11] for normal grain growth, there was till the recent derivation of a growth rate of an embedded polyhedron by McPherson and Srolovitz [19] no benchmark case to validate 3D grain growth models. McPherson and Srolovitz [26] solved analytically the problem of formulating the three dimensional counterpart of the von Neumanns–Mullins law, initially proposed for 2D. The behavior was verified using a FEM-based grain growth model [27]. Also for the present 3D model, the volume change rate $\mathrm{d}V/\mathrm{d}t$ of an embedded grain determined from the simulation dynamics is in excellent agreement with the analytical expression, evaluated on the modeled microstructure [11].

4. Outlook and conclusion

The improved vertex model allows studying the role and consequences of anisotropic grain boundary properties on the resulting microstructure. The model is currently applied to explore the conditions for abnormal grain growth in 3D, varying both the energy and mobility of possible abnormal grains. The first results suggests that the mean field criterion [28] giving an instability line for the occurrence of abnormal grains does overestimate the effect of slight mobility advantages of grains. The simulations show, that a GB energy advantages of 10% may be enough to cause abnormal growth. A systematic study on large grain populations of several thousand grains, difficult to simulate by voxel based techniques, may give more insight on nucleation conditions for abnormal grains. Extending the 3D model further to include boundaries will allow handling realistic grain structures as discussed before in the 2D simplified geometry of the Damascene structure.

A substantial effort exists on extracting GB properties from experimental observation [29]. Recent techniques, such as 3D tomography [30] will give access to three dimensional grain structures at different growth stages. Time resolved experimental microstructures give indirect access to interfacial properties information. Together, these experimental techniques should provide various input data to feed grain growth models. Model simulation based on experimental structures combined with an optimization scheme to generate an interface energy and mobility data-base, which matched best the experimental structure at a later stage, will give new way to develop grain boundary engineering.

References

[1] P. Haasen, Physikalische Metallkunde, 3rd ed., Springer, Berlin, 1994.
[2] J.M. Howe, Interfaces in Materials, Wiley, 1997.
[3] D. Weygand, Y. Bréchet, J. Lépinoux, Phil. Mag. B 78 (1998) 329–352.

[4] D. Weygand, Y. Bréchet, J. Lépinoux, W. Gust, Phil. Mag. B 79 (1999) 703.
[5] D. Weygand, Y. Bréchet, J. Lépinoux, Acta Mater. 47 (1999) 961.
[6] D. Weygand, Y. Bréchet, J. Lépinoux, Phil. Mag. B 80 (2000) 1987.
[7] D. Weygand, Y. Bréchet, J. Lépinoux, Acta Mater. 46 (1998) 6559.
[8] D. Weygand, Y. Bréchet, J. Lépinoux, Interface Sci. 7 (1999) 285.
[9] K. Kawasaki, T. Nagai, K. Nakashima, Phil. Mag. B 60 (1989) 399.
[10] K. Fuchizaki, T. Kusaba, K. Kawasaki, Phil. Mag. B 71 (1995) 333.
[11] M. Syha, D. Weygand, Mod. Sim. Mat. Sci. Eng. 18 (2010) 015010.
[12] H.J. Frost, C.V. Thompson, C.L. Howe, J. Wang, Scripta Metall. 22 (1988) 65.
[13] Z.Z. Du, R.M. McMecking, A.C.F. Cocks, Z. Metallk. 94 (2003) 368.
[14] M. Selzer, D. Weygand, B. Nestler, in preparation.
[15] I. Steinbach, Mod. Sim. Mat. Sci. Eng. 17 (2009) 073001.
[16] N. Moelans, B. Blanpain, P. Wollants, Phys. Rev. Lett. 101 (2008) 025502.
[17] C.S. Smith, Trans. Metall. Soc. A.I.M.E. 175 (1948) 15.
[18] A. Harun, E.A. Holm, M.P. Clode, M.A. Miodownik, Acta Mater. 54 (2006) 3261.
[19] G. Couturier, R. Doherty, C. Maurice, R. Fortunier, Acta Mater. 53 (2005) 977.
[20] Y. Bréchet, J. Phys. III France 4 (1994) 1011.
[21] P.M. Hazzeldine, R.D. Oldershaw, Phil. Mag. A 61 (1990) 579.
[22] J.E. Bailey, P.B. Hirsch, Proc. Roy. Soc. 36 (1997) 11.
[23] D.N. Lee, J. Electronic Materials 32 (2003) 1012.
[24] G. Brunoldi, K.J. Kozaczek, B. Gittleman, T. Marangon, Microelec. Eng. 83 (2006) 2206.
[25] D. Weygand, M. Verdier, J. Lepinoux, Mod. Sim. Mat. Sci. Eng. 17 (2009) 064005.
[26] R.D. MacPherson, D.J. Srolovitz, Nature 446 (2007) 1053–1055.
[27] F. Uyar, S.R. Wilson, J. Gruber, S. Lee, S. Sintay, A. Rollett, D.S. Srolovitz, Int. J. Mat. Res. (2009) 543.
[28] F.J. Humphreys, Acta Mater. 45 (1997) 4231.
[29] A. Rollett, S.B. Lee, R. Campman, G.S. Rohrer, Annu. Rev. Mater. Res. 37 (2007) 627.
[30] W. Ludwig, P. Reischig, A. King, M. Herbig, E.M. Lauridsen, G. Johnson, T.J. Marrow, J.-Y. Buffiere, Rev. Sci. Inst. 80 (3) (2009) 033905.